Journal of Solid State Chemistry 184 (2011) 572–577

Contents lists available at ScienceDirect

Journal of Solid State Chemistry

journal homepage: www.elsevier.com/locate/jssc

Low-compressibility and hard material carbon nitride imide $C_2N_2(NH)$: First principles calculations

Hai-Yan Yan [a], Qun Wei [b,c,*], Bao-bing Zheng [c], Ping Guo [d]

[a] Department of Chemistry and Chemical Engineering, Baoji University of Arts and Sciences, Baoji 721013, PR China
[b] School of Science, Xidian University, Xi'an 710071, PR China
[c] Nonlinear Research Institute, Baoji University of Arts and Sciences, Baoji 721007, PR China
[d] Department of Physics, Northwest University, Xi'an 710069, PR China

ARTICLE INFO

Article history:
Received 24 July 2010
Received in revised form
11 December 2010
Accepted 2 January 2011
Available online 22 January 2011

Keywords:
First principles calculations
Mechanical and electronic properties
Elastic anisotropy
Electronic localization function

ABSTRACT

First principles calculations are performed to investigate the structural, mechanical, and electronic properties of $C_2N_2(NH)$. Our calculated lattice parameters are in good agreement with the experimental data and previous theoretical values. Orthorhombic $C_2N_2(NH)$ phase is found to be mechanically stable at an ambient pressure. Based on the calculated bulk modulus and shear modulus of polycrystalline aggregate, $C_2N_2(NH)$ can be regarded as a potential candidate of ultra-incompressible and hard material. Furthermore, the elastic anisotropy and Debye temperatures are also discussed by investigating the elastic constants and moduli. Density of states and electronic localization function analysis show that the strong C–N covalent bond in CN_4 tetrahedron is the main driving force for the high bulk and shear moduli as well as small Poisson's ratio of $C_2N_2(NH)$.

1. Introduction

Due to the importance in fundamental science and technological applications, searching for ultra-incompressible and superhard materials is an intriguing and long-standing problem [1]. Besides the two well-known superhard materials of diamond and cubic boron nitride (*c*-BN), many experimental and theoretical efforts have been devoted to searching for a new class of hard materials. It is well-known that strong three-dimensional covalent compounds formed by the light elements, namely, B, C, N, and O are good candidates for extraordinary hardness, such as BC_2N [2], BC_5 [3], B_6O [4], etc. Among these covalent compounds, the C–N compounds (C_3N_4, CN, C_3N, etc.) have attracted much attention by boasting high bulk modulus and hardness values comparable with or exceeding than those of diamond. Especially for the β-C_3N_4 phase [5], which has been a particular focus of synthetic work due to the prediction of ultra-high modulus (~430 GPa). Although many researchers have attempted to synthesize crystalline C_xN_y phases by using various techniques, including high-pressure and high-temperature (HP–HT) synthesis; there is still no reliable evidence for analogy of any dense phase of these materials so far. Nonstoichiometric solids with N:C ratios of 1.3–1.5 have been reported in the previous work [6,7]. However, these materials are amorphous or nanocrystalline. Their structures and chemical compositions are not well characterized. Furthermore, the compounds prepared under HP–HT conditions are not generally recovered to ambient conditions.

Recently Horvath-Bordon et al. [8] first synthesized a well-crystallized compound with an N:C ratio of 3:2, carbon nitride imide $C_2N_2(NH)$, in the laser-heated diamond-anvil cell under HP–HT conditions. Single crystal of this new dense carbon nitride phase can be recovered to ambient conditions. By using the TEM, EELS, and SIMS analyses, it was found that $C_2N_2(NH)$ is a defect wurtzite structure, which analogous to that of $Si_2N_2(NH)$. In addition, the bulk modulus of $C_2N_2(NH)$ was calculated to be 277 GPa by the same authors. More recently, this defect wurtzite $C_2N_2(NH)$, synthesized by laser heating from dicyandiamide, has been confirmed again by Synchrotron X-ray diffraction and Raman scattering at high-pressure [9]. On decompression from the high-pressure, there was no phase transition in the sample and the defect wurtzite structure remained at an ambient pressure with a high bulk modulus. However, the detailed physical properties, such as elastic constants, thermodynamic, and electronic properties of this compound are least studied so far. Therefore, as a new kind of carbon nitride phase, one might expect excellent mechanical and other novel physical properties. In the present work, using first principles total energy calculations, we demonstrated that $C_2N_2(NH)$ is a wide band-gap insulator. Moreover the $C_2N_2(NH)$ compound was found to have high bulk modulus and large shear modulus at an ambient pressure. These intriguing properties of $C_2N_2(NH)$ can be attributed

* Corresponding author at: School of Science, Xidian University, Xi'an 710071, PR China.
E-mail address: weiaqun@163.com (Q. Wei).

0022-4596/$ - see front matter © 2011 Elsevier Inc. All rights reserved.
doi:10.1016/j.jssc.2011.01.004

to its unconventional bonding scheme. In addition, $Si_2N_2(NH)$ with the same structure was also studied for comparison.

2. Computational methods

The density functional theory (DFT) [10,11] calculations have been performed within the local density approximation (LDA) [12] and generalized gradient approximation (GGA) [13], as implemented in the Vienna *ab initio* simulation package [14]. The electron and core interactions were included by using the frozen-core all-electron projector augmented wave (PAW) method [15], with H: $1s^1$, C: $2s^22p^2$, N: $2s^22p^3$, and Si: $3s^23p^2$ treated as the valence electrons. The convergence tests used a kinetic energy cutoff of 520 eV for the calculations of two compounds. For the total energy calculations, Monkhorst–Pack k points mesh [16] of $10\times10\times10$ was used for both $C_2N_2(NH)$ and $Si_2N_2(NH)$, which was found to be adequate for obtaining the total energy with an accuracy of about $\sim$ meV/f.u. The elastic constants were calculated from an evaluation of stress tensor generated small strain, and the bulk modulus, shear modulus, Young's modulus, and Poisson's ratio were thus derived from Voigt–Reuss–Hill approximation [17]. Atoms were allowed to relax until Hellman–Feynman forces were <0.001 eV/Å and the maxim strain value was 0.2%.

3. Results and discussion

3.1. Structural properties

Experiments have demonstrated that the solid $C_2N_2(NH)$ at HP–HT ($P>27$ GPa, $T>2000$ K) adopts the space group $Cmc2_1$, which can be recovered to ambient conditions. There are four formula units in the unit cell (see Fig. 1), in which all of the C atoms are tetrahedral coordinated by N atoms, and two inequivalent N1 and N2 atoms are connected to three neighbors with three single covalent bonds. We optimized both lattice geometry and ionic positions to get a fully relaxed structure of $C_2N_2(NH)$ and $Si_2N_2(NH)$. The calculated equilibrium lattice parameters and bond lengths within GGA and LDA methods, together with their corresponding experimental data [8,9,18] and other theoretical values [8,9] are listed in Table 1. It is clear that the predicted lattice constants and bond lengths within the LDA method are smaller than those within the GGA method, as the usual cases. For $C_2N_2(NH)$, the predicted structural constant a, b, and c deviates from the corresponding experimental values within 0.5%, 0.2%, and 0.6%, respectively, and agrees well with the previous theoretical values at an LDA level. Furthermore, it should be noted that the bond lengths are also consistent with those of experimental results in Table 1. For an $Si_2N_2(NH)$, the computed lattice constants are in good agreement with the available experimental data. The maximal error of about 1.2% and 0.9% using LDA and GGA shows the accuracies of our calculations.

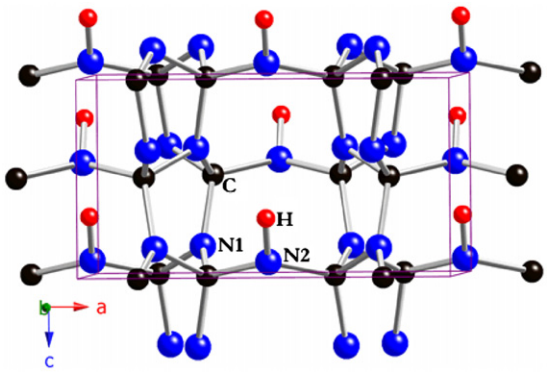

Fig. 1. Crystal structure of $C_2N_2(NH)$, the large, middle, and small spheres represent N, C, and H atoms, respectively.

In order to provide some insight into the pressure behavior of $C_2N_2(NH)$ according to Ref. [9], the total energy of $C_2N_2(NH)$ was minimized as a function of the selected unit cell volume at different pressures. The calculated E–V data were then fitted to the third-order Birch–Murnaghan equation of state [19] (EOS), and we obtained the bulk modulus B_0 and its pressure derivative B_0' to be 256/281 GPa and 3.50/3.49 at GGA/LDA level, respectively. These bulk modulus values are in excellent agreement with the experimental data and other theoretical calculations as shown in Table 1. Moreover the pressure acting on the system as a function of the unit cell volume can be obtained through the thermodynamic relationship given in Ref. [19]. The resulting pressure dependence of the $C_2N_2(NH)$ unit cell is plotted in Fig. 2, along with the experimental data and other theoretical results. Strikingly, the experimental data sit perfectly between curves fitted at GGA and LDA calculations which usually overestimate and underestimate the volumes of crystal, respectively. More interestingly, our DFT calculations within GGA and LDA agree well with the DFT-PBE0 and DFT-B3LYP results [9] separately in Fig. 2. Therefore, the excellent agreements above support the reliability of our calculations in the present work.

3.2. Mechanical properties

3.2.1. Elastic properties

The elastic properties define the behavior of a solid that undergoes stress, deforms, and then recovers and returns to its original shape after stress ceases. To the best of our knowledge, there are

Table 1
Calculated equilibrium lattice parameters, a, b, c, bond length (in Å), EOS fitted Bulk modulus B_0, and its pressure derivative B_0' for $C_2N_2(NH)$ and $Si_2N_2(NH)$.

Structure	Method	a	b	c	B_0	B_0'	$d_{C/Si-N1}$	$d_{C/Si-N2}$	d_{N2-H}
$C_2N_2(NH)$	GGA	7.6827	4.5186	4.0546	256	3.50	1.47, 1.48	1.46	1.06
	LDA	7.5738	4.4429	4.0038	281	3.49	1.45, 1.46	1.44	1.05
	Experimental[a]	7.5362	4.4348	4.0298			1.45, 1.46	1.43	1.05
	Experimental[b]	7.618	4.483	4.038	258	6.3			
	Theoretical[a]	7.5726	4.4425	4.0036					
	Theoretical[b]				271	3.97			
	Theoretical[b]				288	3.94			
$Si_2N_2(NH)$	GGA	9.2720	5.4640	4.8550			1.74, 1.75	1.74	1.03
	LDA	9.1371	5.3437	4.7852			1.72, 1.73	1.72	1.04
	Experimental[c]	9.1930	5.4096	4.8190					

[a] Ref. [8].
[b] Ref. [9].
[c] Ref. [18].

hitherto no available experimental data about the elastic constants of $C_2N_2(NH)$. We hope our work could provide a useful reference for future study. The strain–stress method was used in calculating the elastic constants [20]. A small finite strain was applied on the optimized structure and the atomic position was fully optimized. Then, the elastic constants were obtained from the stress of the strained structure. The calculated elastic constants are listed in Table 2. For stable orthorhombic crystals, the nine independent elastic constants C_{ij} should satisfy the well-known Born stability criteria [21], i.e., $C_{11}>0$, $C_{22}>0$, $C_{33}>0$, $C_{44}>0$, $C_{55}>0$, $C_{66}>0$, $[C_{11}+C_{22}+C_{33}+2(C_{12}+C_{13}+C_{23})]>0$, $(C_{11}+C_{22}-2C_{12})>0$, $(C_{11}+C_{33}-2C_{13})>0$, and $(C_{22}+C_{33}-2C_{23})>0$. Clearly, the calculated elastic constants C_{ij} satisfy Born stability criteria. Thus, the orthorhombic phases of $C_2N_2(NH)$ and $Si_2N_2(NH)$ are all mechanically stable at ambient pressure.

Using the calculated elastic constants C_{ij}, bulk modulus and shear modulus for the corresponding polycrystalline aggregate are thus determined by Voig–Reuss–Hill approximation method [17]. In addition, Young's modulus E_H and Poisson's ratio ν_H are obtained in the light of the following equations:

$$E_H = \frac{9B_HG_H}{3B_H+G_H}, \tag{1}$$

$$\nu_H = \frac{3B_H-2G_H}{6B_H+2G_H}, \tag{2}$$

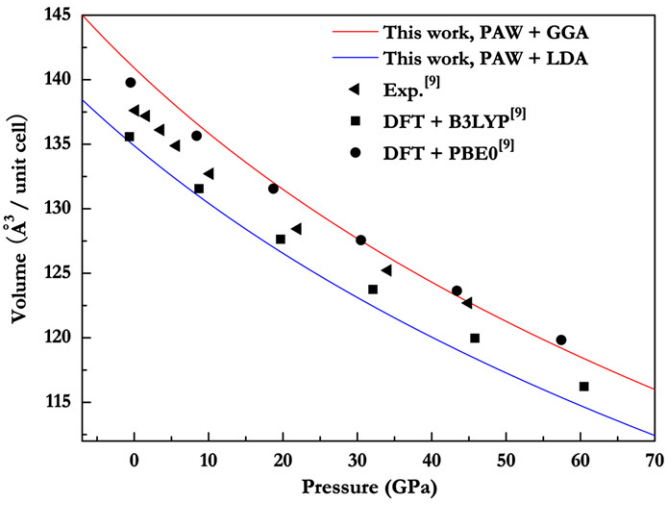

Fig. 2. The pressure dependence of unit cell volume for $C_2N_2(NH)$.

Table 2
Calculated elastic constants C_{ij} (in GPa) for $C_2N_2(NH)$ and $Si_2N_2(NH)$.

Structure	Method	C_{11}	C_{22}	C_{33}	C_{12}	C_{23}	C_{13}	C_{44}	C_{55}	C_{66}
$C_2N_2(NH)$	GGA	597	567	804	89	79	107	335	221	222
	LDA	616	576	871	80	71	103	347	221	218
$Si_2N_2(NH)$	GGA	285	195	313	38	26	43	125	62	75
	LDA	302	255	375	83	47	79	147	86	109

where the subscript H represents Hill approximation. The calculated bulk modulus, shear modulus, Young's modulus, and Poisson's ratio are given in Table 3. The calculated bulk modulus of $C_2N_2(NH)$ is 276/282 GPa at the GGA/LDA level, which is close to the experimental data of B_6O (270 GPa) [22], indicating ultra-incompressible character. In addition, these calculated bulk moduli agree well with those directly obtained from the fitting of the third-order Birch–Murnaghan EOS listed in Table 1, which further demonstrates the reliability of our calculations. As a better indicator of the potential hardness for materials, shear modulus quantifies the resistance to the shear deformation. Remarkably, the calculated shear modulus is very large for $C_2N_2(NH)$, 265 GPa within GGA and 270 GPa within an LDA. Thus, it is expected to withstand shear strain to a large extent. In addition, the relative directionality of the bonding in the material also has an important effect on its hardness and can be determined by the G/B ratio. The calculated ratio G/B for $C_2N_2(NH)$ is 0.960, which is slightly smaller than that of diamond (1.10) and close to that of α-C_3N_2 (0.96) and β-C_3N_2 (1.07) at the GGA level [23]. This shows that there exists strong directionality in the C–N bond. All these excellent mechanical properties strongly suggest that $C_2N_2(NH)$ is a potential candidate to be ultra-incompressible and hard. Comparing with $C_2N_2(NH)$, the elastic moduli of $Si_2N_2(NH)$ are remarkably lower, which may be due to the weaker directionality of the Si–N bond, as shown in Table 3.

3.2.2. Elastic anisotropy

The elastic anisotropy of crystals can exert great effects on the properties of physical mechanism, such as anisotropic plastic deformation, crack behavior, and elastic instability. Hence, it is important to calculate elastic anisotropy in order to improve its mechanical durability [24]. The shear anisotropic factors provide a measure of the degree of anisotropy in the bonding between atoms in different planes. The shear anisotropic factor for the {1 0 0} shear planes between the ⟨0 1 1⟩ and ⟨0 1 0⟩ directions is

$$A_1 = \frac{4C_{44}}{C_{11}+C_{33}-2C_{13}}. \tag{3}$$

For the {0 1 0}, shear planes between the ⟨1 0 1⟩ and ⟨0 0 1⟩ directions it is

$$A_2 = \frac{4C_{55}}{C_{22}+C_{33}-2C_{23}}, \tag{4}$$

and for the {0 0 1} shear planes between the ⟨1 1 0⟩ and ⟨0 1 0⟩ directions it is

$$A_3 = \frac{4C_{66}}{C_{11}+C_{22}-2C_{12}}. \tag{5}$$

For an isotropic crystal, the factors A_1, A_2, and A_3 must be 1.0, while any value smaller or greater than 1.0 is a measure of the degree of elastic anisotropy. Moreover for an orthorhombic crystal, the elastic anisotropy which arises from the anisotropy of linear bulk modulus was also considered in addition to the shear anisotropy. The anisotropy of the bulk modulus along the a- and c-axis with respect to the b-axis are given by $A_{Ba}=(B_a/B_b)$

Table 3
Calculated bulk modulus B, shear modulus G, Young's modulus E (in GPa), Poisson's ratio V, B/G ratio, and Debye temperature T_D (K) of $C_2N_2(NH)$ and $Si_2N_2(NH)$.

Structure	Method	B_V	B_R	B_H	G_V	G_R	G_H	E_H	ν	G_H/B_H	T_D
$C_2N_2(NH)$	GGA	280	272	276	269	260	265	600	0.137	0.960	1658
	LDA	286	277	282	275	265	270	616	0.135	0.957	1662
	Theoretical[a]			277							
$Si_2N_2(NH)$	GGA	112	107	110	98	90	94	220	0.166	0.855	894
	LDA	150	144	147	117	111	114	272	0.192	0.776	978

[a] Ref. [8].

and $A_{Bc}=(B_c/B_b)$, where B_a, B_b, and B_c are the bulk modulus along different crystal axes, defined as $B_i=i(dP/di)$, $i=a$, b, and c. Note that a value of 1.0 indicates an elastic isotropy and any deviation from 1.0 represents an elastic anisotropy. In addition, we also calculated the percentage elastic anisotropy for shear modulus A_G and bulk modulus A_B in polycrystalline materials, which can be defined as follows: $A_G=((G_V-G_R)/(G_V+G_R))$ and $A_B=((B_V-B_R)/(B_V+B_R))$, where the subscripts V and R represent the Voit and Reuss approximations. The implication of the definition is that a value of zero corresponds to an elastic isotropy, and a value of 100% identifies the largest elastic anisotropy.

Using the relations mentioned above, the parameters about an elastic anisotropy are calculated and only the values of $C_2N_2(NH)$ are shown in Table 4 for simplicity. It is clear that the $C_2N_2(NH)$ is an elastic anisotropic. The shear anisotropy results indicate that the an elastic anisotropy for {0 1 0} shear planes between the ⟨1 0 1⟩ and ⟨0 0 1⟩ directions is larger than those for the {1 0 0} shear planes between the ⟨0 1 1⟩ and ⟨0 1 0⟩ directions and the {0 0 1} shear planes between the ⟨1 1 0⟩ and ⟨0 1 0⟩ directions. Moreover it is interesting to note that the directional bulk modulus along the c-axis is larger than those along the a- and b-axis, which is consistent with the predicted elastic constants along different axes (see Table 2). In addition, we also noticed that the percentage shear modulus A_G (1.89%/2.39% within GGA/LDA) is bigger than the percentage bulk modulus A_B (1.45%/1.78% within GGA/LDA), indicating that there is more anisotropy in shear than in compressibility for $C_2N_2(NH)$.

As a fundamental parameter, Debye temperature closely relates to many physical properties of solids, such as specific, dynamic properties, and melting temperature [24]. At low temperature, it can be calculated from the elastic constants, using the average sound velocity v_m, by the following equation

$$\Theta_D=\frac{h}{k}\left[\frac{3n}{4\pi}\left(\frac{\rho N_A}{M}\right)\right]^{1/3}v_m, \tag{6}$$

where h is Planck's constant, k is Boltzmann's constant, N_A is Avogadro's number, n is the number of atoms per formula unit, M is the molecular mass per formula unit, and ρ is the density. The average sound velocity v_m is given by

$$v_m=\left[\frac{1}{3}\left(\frac{2}{v_t^3}+\frac{1}{v_l^3}\right)\right]^{-(1/3)}, \tag{7}$$

where v_t and v_l are the transverse and longitudinal elastic wave velocities of the polycrystalline materials and are given by Navier's equation [25]. The calculated values of Debye temperatures are listed in Table 3. Our results have predicted that T_D of $C_2N_2(NH)$ is higher than that of an $Si_2N_2(NH)$. This shows that

Table 4
Calculated anisotropy factors A_1, A_2, A_3, A_{Ba}, A_{Bc}, A_G, A_B and directional bulk modulus B_a, B_b, B_c (in GPa) of $C_2N_2(NH)$.

Structure	Method	A_1	A_2	A_3	A_{Ba}	A_{Bc}	B_a	B_b	B_c	A_G	A_B
$C_2N_2(NH)$	GGA	1.1289	0.7288	0.9052	1.060	1.476	760.1	716.8	1058.3	1.89%	1.45%
	LDA	1.0835	0.6774	0.8450	1.124	1.651	776.1	690.1	1139.4	2.39%	1.78%

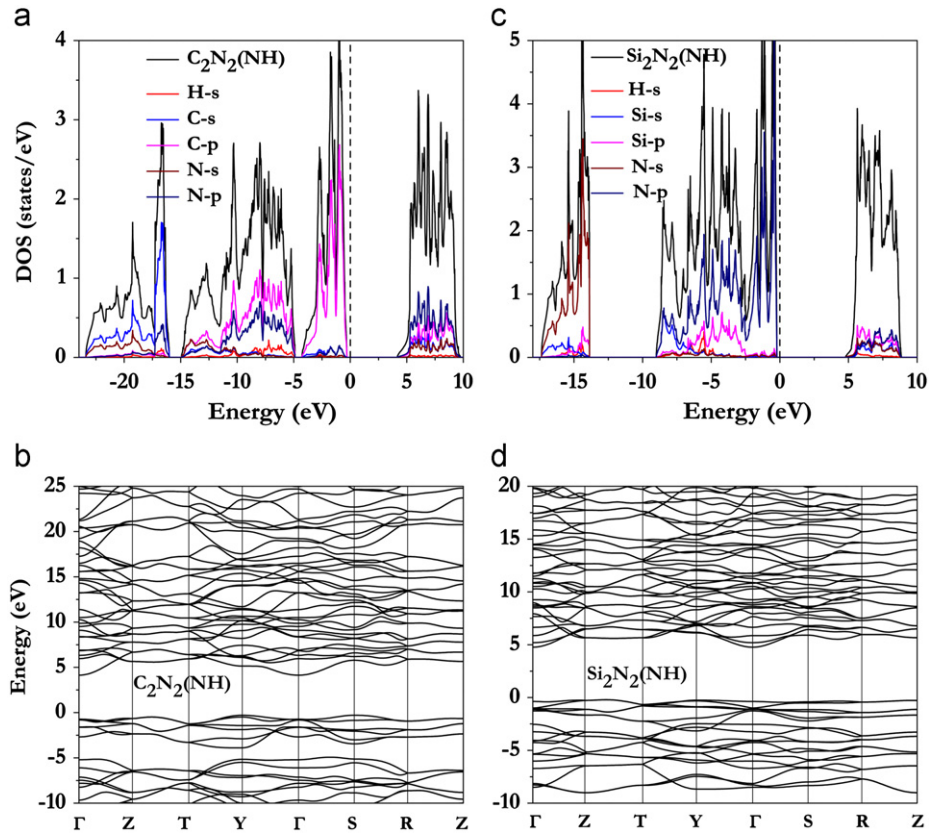

Fig. 3. The calculated total and partial density of state (a), electronic band structure (b) of $C_2N_2(NH)$, total and partial density of state (c), and electronic band structure (d) of $Si_2N_2(NH)$.

$C_2N_2(NH)$ is harder than an $Si_2N_2(NH)$. For both compounds, due to the tendency to overestimate the bonding, the calculated results obtained within LDA are slightly larger than those within GGA.

3.3. Electronic properties

3.3.1. Band structure and density of states

To gain a deeper insight into the elastic properties, the band structures and electronic densities of states (DOS) of $C_2N_2(NH)$ and $Si_2N_2(NH)$ were calculated at zero pressure within the GGA method, as shown in Fig. 3. Both compounds are insulators characterized by large energy gap of ~4.36 eV for $C_2N_2(NH)$ and ~5.01 eV for $Si_2N_2(NH)$ (see Fig. 3b and d). As is well-known, the band gap is generally underestimated within density functional calculations at least about 30%, so the true band gap may be larger than 5.67 and 6.51 eV, leading to excellent optical applications. The atom-resolved PDOS of $C_2N_2(NH)$ and $Si_2N_2(NH)$ is plotted in Fig. 3a and c, respectively. The main features of $C_2N_2(NH)$ can be summarized as follows: (a) the peak present in the lower energy part of the DOS curve, which is mainly due to contributions of the *s* electrons of C and N; (b) the bonding states of C-*s*, *p* and N-*s*, *p* orbitals near Fermi level; (c) the top of DOS curve due to the antibonding states. It is found that the part *s* electrons of C and N are localized in the low energy range −23 to −16 eV. The electrons from C-*s* and C-*p* orbitals have a significant hybridization with N-*s* and N-*p* orbitals from the −15 eV up to Fermi level, signifying the strong C–N covalent bonding nature in the CN_4 tetrahedrons, which has been further confirmed by the following electronic localization function (ELF) calculations [26,27]. In the conduction band region of DOS, the peaks are mainly superimposed by the C-*p* and N-*p* states. For an $Si_2N_2(NH)$ compound, similar trend can be observed (see Fig. 3c).

Table 5
Calculated charge transfer among different atoms in the $C_2N_2(NH)$ and $Si_2N_2(NH)$.

Structure		*s*	*p*	Total	Charge
$C_2N_2(NH)$	H	0.6	0.0	0.6	0.4
	C (× 2)	1.01	2.56	3.57	0.43
	N1 (× 2)	1.40	3.95	5.36	−0.36
	N2	1.47	4.08	5.55	−0.55
$Si_2N_2(NH)$	H	0.6	0.0	0.6	0.4
	Si (× 2)	0.79	1.39	2.18	1.82
	N1 (× 2)	1.66	4.71	6.37	−1.37
	N2	1.65	4.66	6.30	−1.30

The bonding mechanism of these two compounds can be further analyzed by examining the charge transfer situation by Mulliken atomic population analysis, which is useful in evaluating the nature bonds in a compound. Although the absolute magnitudes of Mulliken populations have little physical meaning, the relative values can still offer some useful information [28]. The charge transfer values for $C_2N_2(NH)$ and $Si_2N_2(NH)$ are shown in Table 5, in which the N1 and N2 are two inequivalent atoms demonstrated in Fig. 1. The total valences for C and Si in the two solids are 3.57 and 2.81, unequal to 4; moreover the Si atoms have 6.30–6.37 electrons, larger than those of C atoms in $C_2N_2(NH)$. These values show that these compounds also possess an ionic feature. We also noted that the charge transfer from H to N is 0.4*e* in two compounds. Compared to the values of charge transfer (0.86*e*) from C to N atoms in $C_2N_2(NH)$, Si atoms have more charge transfer (3.64*e*) to N, which mainly come from the Si-2*s* orbital in an $Si_2N_2(NH)$. Therefore, the Si–N bond has more ionicity than that of the C–N bond, which may be responsible

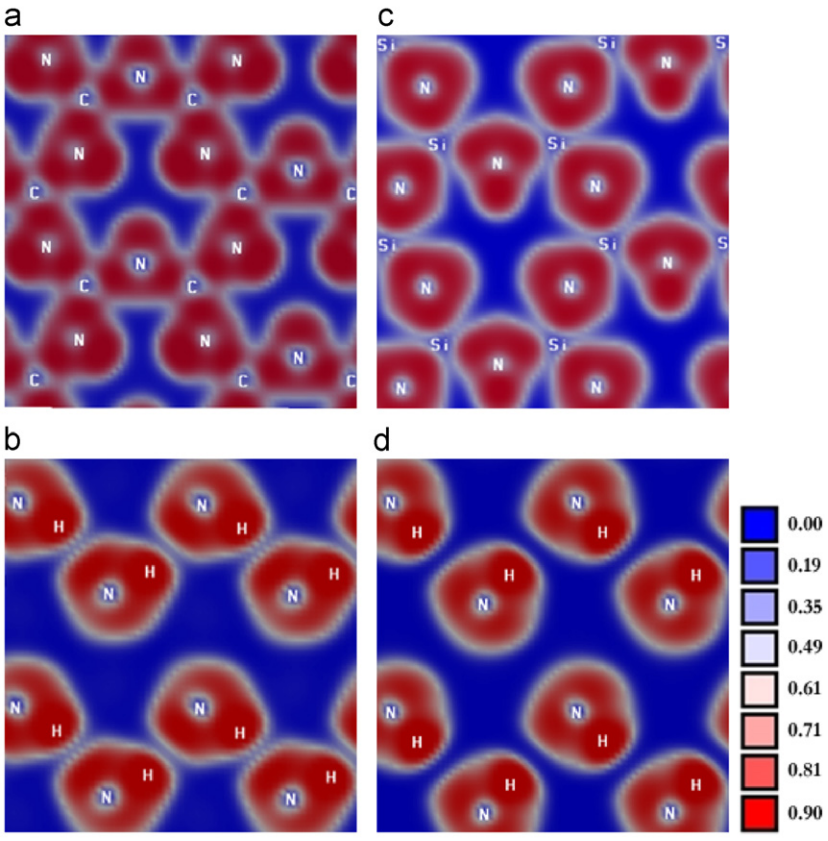

Fig. 4. Contours of electronic localization function (ELF) of $C_2N_2(NH)$ on the: (0 0 1) plane (a), (1 0 0) plane (b), ELF of $Si_2N_2(NH)$ on the: (0 0 1) plane (c), and (1 0 0) plane (d).

for the lower elastic moduli of an $Si_2N_2(NH)$. We thus conclude that the chemical bonding in these two solids is a complex mixture of covalent and ionic characters.

3.3.2. Electronic localization function analysis

In order to quantitatively identify the chemical bond character in two compounds, we have calculated the ELF, which is a measure of the probability of finding an electron near another electron with the same spin. The ELF is represented as a contour plot in real space, where different contours correspond to numerical values ranging 0.0–1.0. In the region with an ELF is 1.0, there is no chance of finding two electrons with the same spin. This usually occurs in places, where bonding pairs molecular orbitals or lone pairs atomic orbitals reside. An ELF 0.0 corresponds to the area, where there is no electron density, and a homogeneous electron gas, like in metals, ELF is 0.5. It should be noted that an ELF is a measure of Pauli principle and not of an electron density [29]. The contours of ELF domains for the $C_2N_2(NH)$ and $Si_2N_2(NH)$ on their respective crystal plane are shown in Fig. 4. For $C_2N_2(NH)$, we note strong C–N covalent bonds on the (0 0 1) plane, with nearly identical C–N covalent "point attractors" at ELF=0.9. At the (1 0 0) plane, the ELF is negligible at the *N* sites, whereas it attains local maximum values at the *H* sites, manifesting another covalent interaction between N and H atoms. The bonding situation in $Si_2N_2(NH)$ is similar to that seen for $C_2N_2(NH)$ in Fig. 4c. However, in contrast, covalent interaction between C and N in $C_2N_2(NH)$ is stronger than that between Si and N in $Si_2N_2(NH)$, which is the main driving force for its higher bulk and shear modulus.

4. Conclusions

Based on the first principles calculations, we have investigated the mechanical and electronic properties of $C_2N_2(NH)$ and $Si_2N_2(NH)$. Our calculated lattice parameters are in good agreement with the experimental data and previous theoretical values. The predicted high bulk modulus and large shear modulus suggested that $C_2N_2(NH)$ is a potential low compressible and hard material. Meanwhile, $C_2N_2(NH)$ compound shows different degrees of an elastic anisotropy. Moreover both $C_2N_2(NH)$ and $Si_2N_2(NH)$ are found to have insulating feature with large band gaps of $\sim$4.36 and $\sim$5.01 eV. In addition, our electronic densities of states and electronic localization function calculations confirmed that the strong covalent C–N bonding in CN_4 tetrahedrons play a key role in the incompressibility and hardness of $C_2N_2(NH)$. We hope that these calculations will be helpful for future experimental works on these technologically important materials.

Acknowledgments

This work is supported by the Education Committee Natural Science Foundation of Shaanxi Province (Grant no. 2010JK404) and Baoji University of Arts and Sciences Key Research (Grant no. ZK0915, ZK0918).

References

[1] R.B. Kaner, J.J. Gilman, S.H. Tolbert, Science 308 (2005) 1268.
[2] V.L. Solozhenko, D. Andrault, G. Fiquet, M. Mezouar, D.C. Rubie, Appl. Phys. Lett. 78 (2001) 1385.
[3] V.L. Solozhenko, O.O. Kurakevych, D. Andrault, Y.L. Godec, M. Mezouar, Phys. Rev. Lett. 102 (2009) 015506.
[4] D.W. He, Y. Zhao, L. Daemen, J. Qian, T.D. Shen, T.W. Zerda, Appl. Phys. Lett. 81 (2002) 643.
[5] A.Y. Liu, M.L. Cohen, Science 245 (1989) 841.
[6] E. Horvath-Bordon, R. Riedel, A. Zerr, P.F. McMillan, G. Auffermann, Y. Prots, W. Bronger, R. Kniep, P. Kroll, Chem. Soc. Rev. 35 (2006) 987.
[7] E. Kroke, M. Schwarz, Coord. Chem. Rev. 248 (2004) 493.
[8] E. Horvath-Bordon, R. Riedel, P.F. McMillan, P. Kroll, G.M.A.v. Aken, A. Zerr, P. Hoppe, O. Shebanova, I. McLaren, S. Lauterbach, E. Kroke, R. Boehler, Angew. Chem. Int. Ed. 46 (2007) 1476–1480.
[9] A. Salamat, K. Woodhead, P.F. McMillan, R.Q. Cabrera, A. Rahman, D. Adriaens, F. Cora, J.-P. Perrillat, Phys. Rev. B 80 (2009) 104106.
[10] P. Hohenberg, W. Kohn, Phys. Rev. 136 (1964) B864.
[11] W. Kohn, L.J. Sham, Phys. Rev. 140 (1965) A1133.
[12] D.M. Ceperley, B.J. Alder, Phys. Rev. Lett. 45 (1980) 566.
[13] J.P. Perdew, K. Burke, M. Ernzerhof, Phys. Rev. Lett. 77 (1996) 3865.
[14] G. Kresse, D. Joubert, Phys. Rev. B 59 (1999) 1758.
[15] P.E. Blchl, Phys. Rev. B 50 (1994) 17953.
[16] J.D. Pack, H.J. Monkhorst, Phys. Rev. B 16 (1977) 1748.
[17] R. Hill, in: Proc. Phys. Soc. London 65 (1952) 349.
[18] D. Peters, H. Jacobs, J. Less-Common Met. 146 (1989) 241.
[19] F. Birch, Phys. Rev. 71 (1947) 809.
[20] V. Milman, M.C. Warren, J. Phys., Condens. Matter 13 (2001) 241.
[21] M. Born, Proc. Cambridge Philos. Soc. 36 (1940) 160.
[22] D. He, S.R. Shieh, T.S. Duffy, Phys. Rev. B 70 (2004) 184121.
[23] F. Tian, J. Wang, Z. He, Y. Ma, L. Wang, T. Cui, C. Chen, B. Liu, G. Zou, Phys. Rev. B 78 (2008) 235431.
[24] P. Ravindran, L. Fast, P.A. Korzhavyi, B. Johansson, J. Wills, O. Eriksson, J. Appl. Phys. 84 (1998) 4891.
[25] E. Schreiber, O.L. Anderson, N. Soga, Elastic Constants and their Measurements, McGraw-Hill, New York, 1973.
[26] A.D. Becke, K.E. Edgecombe, J. Chem. Phys. 92 (1990) 5397.
[27] A. Savin, B. Silvi, Nature 371 (1994) 683.
[28] M.D. Segall, R. Shah, C.J. Pickard, M.C. Payne, Phys. Rev. B 54 (1996) 16317.
[29] N. Ooi, A. Rairkar, L. Lindsley, J.B. Adams, J. Phys.: Condens. Matter 18 (2006) 97.